



Contents lists available at [SciVerse ScienceDirect](#)

Electrochimica Acta

journal homepage: www.elsevier.com/locate/electacta



Saccharin effect on properties of 2.4 T CoFe films

Stanko R. Brankovic^{a,b,*}

^a Electrical and Computer Engineering Department, University of Houston, Houston, TX 77204, United States

^b Chemical and Biomolecular Engineering Department, University of Houston, Houston, TX 77204, United States

ARTICLE INFO

Article history:

Received 23 May 2012

Received in revised form 17 July 2012

Accepted 17 July 2012

Available online xxx

Keywords:

CoFe films

Saccharin

Electrodeposition

Additives

ABSTRACT

The current trends in magnetic device designs favor the electrodeposited 2.4 T CoFe films due to their ultimately high magnetic moment and relatively low coercivity. The optimum properties of these films are largely function of the additive design in the electrodeposition solution. Saccharin is the most commonly used one and, for this reason, the focus in this article is on reviewing the current understanding and phenomenological description of saccharin effects on properties of electrodeposited 2.4 T CoFe films.

© 2012 Elsevier Ltd. All rights reserved.

1. Introduction

The recent trends in magnetic recording and Micro-Electro-Mechanical System (MEMS) technologies indicate that electrodeposited Soft High Magnetic Moment (SHMM) alloys will be the material of choice for fabrication of future magnetic devices [1–3]. The current research in this area focuses toward synthesis of ultimately soft magnetic alloys with the maximum possible magnetic moment (2.4 T CoFe alloys), good corrosion resistance and low stress levels [3]. This seemingly difficult challenge is coupled with the ever-continuing drive to miniaturize magnetic devices, bringing the electrodeposition to the level of nano-science [4,5]. Researchers in industry and academia are facing the task of delivering controlled process and properties of SHMM alloys into lithographically defined patterns and nanoscale electrode geometries with sub-micron dimensions [6].

In order to obtain magnetic alloys with low coercivity, different additives have been used in design of the electrodeposition solutions [7–11]. The general action of additives is expressed through the leveling and brightening of the deposit, improved crystal structure [1,3,12], refined grain size [9,10] and lower residual stresses [13–15]. The presence of additives in the electrodeposition solutions results in their incorporation into magnetic deposit [15–20]. If the amount of incorporated additives is small, it is generally considered as beneficial [10,16].

However, the significant presence of sulfur, metal sulfides, or S-containing organic molecules in magnetic deposit can have a detrimental effect on alloy corrosion resistance [21]. Because of that, the benefit and disadvantage of additives for overall properties of magnetic alloys have to be considered with great attention.

The current magnetic device designs favor the use of electrodeposited 2.4 T CoFe films (CoFe films in further text) due to their ultimately high magnetic moment [1,3]. Their optimum properties are largely function of the additive design in the solution. The saccharin is the most commonly used one and this article is reviewing the current understanding and phenomenological description of the saccharin effects on properties of the electrodeposited CoFe films.

2. Saccharin adsorption and incorporation phenomenon

Saccharin represents condensed organic molecule having the benzene and heterocyclic rings in its structure. As an additive, saccharin adsorbs on the metal/deposit surface forming a condensed phase [22]. Its molecule has very small dipole moment causing saccharin adsorption to be the strongest in the region around potential of zero charge (PZC). The density and coverage of adsorbed saccharin phase are dependent on the potential of electrode surface and its concentration in the solution [23]. The information about saccharin coverage (θ) is obtained from the electrochemical impedance spectroscopy (EIS) measurements of the double layer capacity [24]. The example of EIS measurements for CoFe surface in saccharin containing solutions is shown in Fig. 1A [3]. From known C_{DL} vs. E dependence, the corresponding saccharin coverage as a function

* Correspondence address. Electrical Engineering Department, N308, Engineering Bldg. 1, University of Houston, Houston, TX 77204–4005, United States.

E-mail address: Stanko.Brankovic@mail.uh.edu

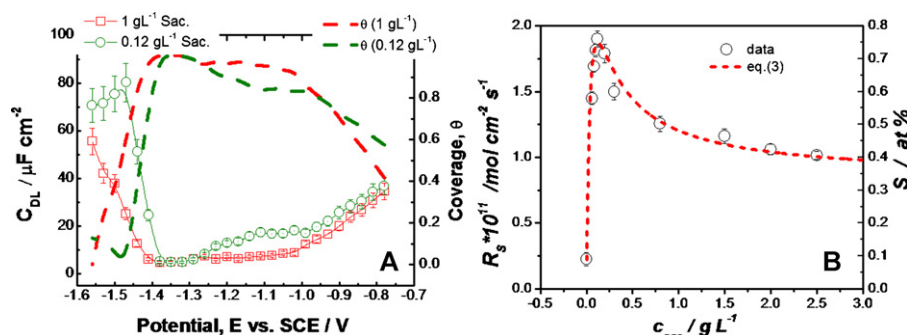


Fig. 1. (A) The double layer capacitance as a function of potential extracted from the EIS measurements for CoFe surface in solution with different saccharin concentrations. Background solution: 0.3 M NH_4Cl + 0.4 M H_3BO_3 , pH = 2.1 [3]. (B) Incorporation rate of sulfur (R_S) as function of c_{sac} for CoFe films. The right ordinate in (B) shows corresponding sulfur content in the alloy. Electrodeposition conditions and solution design: 0.1 M $FeSO_4$ + 0.05 M $CoSO_4$ + 0.3 M NH_4Cl + 0.4 M H_3BO_3 , pH = 2.1. ω = 300 rpm and j = 4 mA cm^{-2} [18].

of the electrode potential is calculated using well-known Frumkin relation [24], Fig. 1A;

$$\theta(E) = \frac{C_{DL}^{max} - C_{DL}(E)}{C_{DL}^{max} - C_{DL}^{min}} \quad (1)$$

Here, C_{DL}^{max} and C_{DL}^{min} represent the maximum and the minimum value of the double layer capacitance for the potential range of interest and the term, $C_{DL}(E)$, is the double layer capacitance at potential for which the saccharin coverage is considered. For CoFe surface, the maximum in saccharin coverage is observed at potential of ≈ -1.33 V vs. SCE. This potential is slightly more negative than the PZC for individual Fe, or Co metals [25]. At constant electrode potential, the saccharin coverage is expressed as a function of its concentration in the solution (c_{sac}) using Langmuir adsorption formalism [26];

$$\theta(c_{sac}) = \frac{b \cdot c_{sac}}{1 + b \cdot c_{sac}} \quad (2)$$

Here, the b term represents the saccharin equilibrium adsorption constant. Evidently, choosing the potential of the electrode surface or saccharin concentration in the solution one effectively controls the saccharin coverage on CoFe surface during electrodeposition process. The control of saccharin coverage means direct control of its action as an additive.

The sulfur atom is the integral part of the saccharin molecule. It can be used as a tracer element to investigate the amount/rate of saccharin incorporation into the CoFe deposit. The sulfur incorporation coming from the saccharin occurs either via saccharin adsorption–electroreduction process or via physical incorporation of the entire saccharin molecules [18,20]. The first mechanism represents the chemical route responsible for incorporation of metal–sulfides, while the second one represents entrapment of the entire saccharin molecules having the sulfur atom as their integral part. The physical entrapment of sulfur containing ions is additional source of sulfur in magnetic deposit, independent on saccharin presence in the solution. The overall sulfur incorporation rate into magnetic films, R_S [mol $cm^{-2} s^{-1}$], is the sum of the contributions coming from each of the three mentioned sources [3]. Its dependence on saccharin concentration, c_{sac} , can be expressed as [20];

$$R_S = R_0 + K_1 \cdot \frac{b \cdot c_{sac}}{1 + b \cdot c_{sac}} + K_2 \cdot \frac{b \cdot c_{sac}}{(1 + b \cdot c_{sac})^2} \quad (3)$$

The first term on the right side, R_0 , represents the sulfur incorporation as a part of trapped anions in the deposit. The second term represent the sulfur incorporation via electroreduction of saccharin molecules [20]. The last term, represents the sulfur incorporation as a part of physically trapped saccharin

molecules [18]. The K_1 and K_2 are the saccharin electroreduction and physical incorporation rate constants. The fit of Eq. (3) to the experimental data for CoFe films is shown in Fig. 1B [3,20].

The inspection of Eq. (3) suggests that for $c_{sac} \ll (K_2 - K_1)/K_1 \cdot b$ the sulfur incorporation into magnetic deposit is mainly as a part of saccharin molecules. For $c_{sac} \gg (K_2 - K_1)/K_1 \cdot b$ the sulfur incorporates into deposit mainly as a part of metal sulfides [3]. The data and model fit presented in Fig. 1B provide opportunity to extract the values of K_1 , K_2 and b constants for particular solution formulation and deposition conditions (potential/current, cell geometry, and transport). This way, the quantitative assessment of the saccharin incorporation dependence on the particular conditions of electrodeposition process can be studied. Eq. (3) also provides phenomenological description of the incorporation process of other atoms or atomic groups originating from saccharin molecule. For example, the incorporation rate of carbon or nitrogen, constituents of saccharin molecule, is expected to follow the same functional dependence presented by Eq. (3) [3,16].

3. Saccharin effect on coercivity of CoFe films

Many authors have discussed the effect of saccharin on coercivity of CoFe films [1,3,15,18]. The typical data showing CoFe alloy coercivity dependence on saccharin concentration are shown in Fig. 2A [15,20]. This dependence is different from the one reported for the CoNiFe and NiFe films [12,27–29]. Rather than monotone decrease of H_c or $H_c \approx \text{const}$ for an increasing c_{sac} , in the case of CoFe films, a more complex H_c vs. c_{sac} dependence is observed [15,18]. The largest values of coercivity are obtained for CoFe films electrodeposited from saccharin-free solution. The small additions of this additive in the electrodeposition bath result in significant decreases of H_c [15,18]. The lowest coercivity is achieved for certain threshold value of saccharin concentration (0.12 g/L) after which an increasing saccharin concentration results in CoFe films with higher H_c values. The useful analysis of the results in Fig. 2A is made if the H_c values are presented against the sulfur incorporation rate coming from saccharin incorporation phenomenon, Fig. 2B. From this analysis, it is obvious that the higher incorporation rates of sulfur/saccharin decrease CoFe alloy's coercivity. The important conclusion is deduced if the H_c data in Fig. 2A are plotted as a function of the ratio between the sulfur incorporation rate coming from the physical incorporation of saccharin molecules ($R_M = K_2 \cdot ((b \cdot c_{sac})/(1 + b \cdot c_{sac})^2)$) and sulfur incorporation rate coming from the saccharin electroreduction ($R_{ER} = K_1 \cdot ((b \cdot c_{sac})/(1 + b \cdot c_{sac}))$) [20]. This analysis suggests that, as long as R_M represents the dominant contribution to the overall sulfur content in CoFe films, $R_M/R_{ER} \gg 1$, the coercivity of electrodeposited films has the lower (optimum)

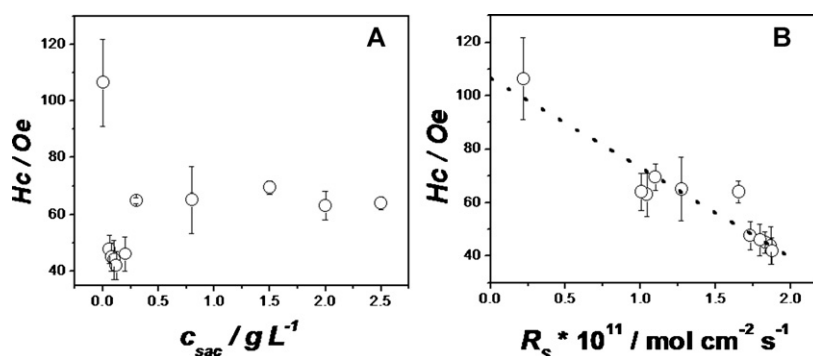


Fig. 2. (A) Coercivity vs. c_{sac} and (B) coercivity vs. R_s for electrodeposited CoFe films. The substrate in this study is electropolished polycrystalline Cu disk. The parameters of the electrodeposition process and solution are: 0.1 M $FeSO_4$ + 0.05 M $CoSO_4$ + 0.3 M NH_4Cl + 0.4 M H_3BO_3 , pH = 2.1. ω = 300 rpm and j = 4 mA cm⁻² [3,20].

values. In the case where R_{ER} makes predominant contribution to the sulfur content in the deposit, $R_M/R_{ER} \leq 1$, the CoFe films' coercivity has significantly higher values. Therefore, the most effective form of incorporated sulfur producing the soft CoFe films is the sulfur as part of saccharin molecule. The incorporated sulfur as part of metal sulfides also contributes to the decrease in coercivity but less effectively. The optimum design of electrodeposition solutions for ultimately soft CoFe films has to satisfy $R_M \gg R_{ER}$ criterion [3].

4. Saccharin effect on stress in CoFe films

The CoFe films express a tensile stress in "as deposited" state which significantly alters their magnetic properties [1,3,14]. The magnetic anisotropy energy of these films is a strong function of magnetoelastic energy and small alterations in stress level can produce significant change in their magnetic anisotropy and coercivity [1,14]. The sulfur bearing additives such as saccharin are effective stress relieving agents [1,3]. Saccharin adsorbs on CoFe surface during electrodeposition [6,16,22] and modifies the thermodynamics of nucleation and grain boundary formation [14,31]. Saccharin incorporates into electrodeposited CoFe films in a form of a low surface energy phase [10,16,16,20] and segregates at the grain boundaries affecting their specific energy during grain zipping and grain coalescence process [1,30,31]. There are various reports in literature about the additive concentration effect on the level of growth stress in electrodeposited magnetic alloys/films. The most of the reports studying saccharin are obtained using ex situ wafer curvature measurements [3,15]. The observed stress is found to be a decreasing function saccharin concentration [14,15,31].

In Fig. 3A, the maximum growth stress of the electrodeposited CoFe films as a function of saccharin concentration is presented

[30,31]. These data are obtained from in situ cantilever bending measurements [32] where the average stress acting on the cross-section of the film is calculated from cantilever curvature using Stony's equation [33]. The stress-thickness profile (not shown) indicates that CoFe films represent a low ad-atom mobility system where the maximum tensile stress is set during the grain zipping process [34–38]. The saccharin action as a stress reliever during electrodeposition of CoFe films is mainly confined to the mitigation of the grain zipping process. This is achieved through the saccharin adsorption on growing CoFe surface which modifies the surface energy of the zipping CoFe grains, and consequently the grain boundary energy of newly formed grain boundaries [30,31]. The analytical model based on this assumption is presented below. The model fit, Eq. (4), to the experimental data is shown in Fig. 3A with dotted line [31].

$$\sigma_{AVRG}^{max}(c_{sac}) = \sigma_{AVRG,CoFe}^{max} - 8 \frac{\Delta\gamma^*}{d_G} \cdot \frac{b \cdot c_{sac}}{1 + b \cdot c_{sac}} \quad (4)$$

The physical meaning of $\Delta\gamma^*$ term in above expression is the difference in driving force for zipping of CoFe grains with "saccharin-free" surface and CoFe grains with the maximum coverage of adsorbed saccharin phase ($\theta = 1$). The $\sigma_{AVRG,CoFe}^{max}$ is the maximum tensile stress in CoFe films electrodeposited from saccharin-free solution while d_G represents the average diameter of CoFe grains. Depending on the electrodeposition conditions and solution formulation, d_G can be *const.* [31] ($d_G \neq f(c_{sac})$), or it could have a more complex dependence on saccharin concentration, ($d_G = f(c_{sac})$) [15]. The second term on the right side of Eq. (4) represents the reduction of the stress due to the presence of saccharin adsorbed phase on CoFe surface.

The effect of growth stress on coercivity of in CoFe films is shown in Fig. 3B [31]. The largest coercivity was found for the

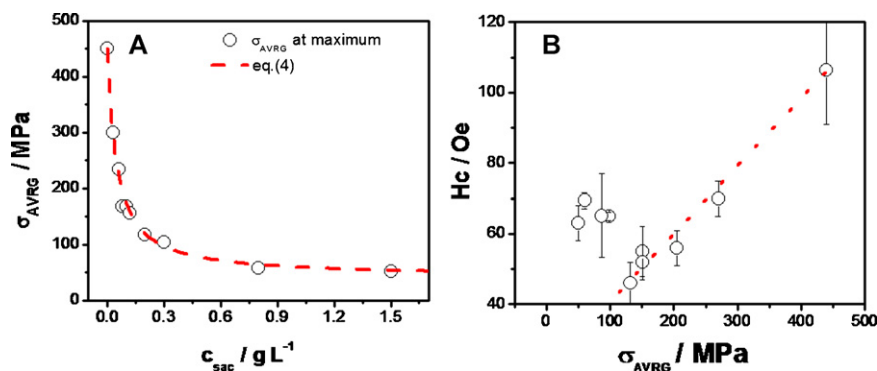


Fig. 3. (A) The maximum average stress in CoFe films as function of saccharin concentration in solution. The dashed line is the model fit, Eq. (4), to the experimental data. (B) Coercivity dependence on growth stress for 0.3×10^{-6} m thick CoFe films. The solid line is to guide an eye [31]. The electrodeposition condition and solution are: 0.1 M $FeSO_4$ + 0.05 M $CoSO_4$ + 0.3 M NH_4Cl + 0.4 M H_3BO_3 , pH = 2.1. ω = 0 rpm and j = 4 mA cm⁻². The CoFe films are deposited on 100 nm Au films evaporated on glass cantilevers.

sample with correspondingly highest level of stress (electrodeposited from saccharin-free solution, $\sigma_{\text{AVRG}} = 420 \times 10^6$ Pa, $H_c = 110$ Oe). The decrease in σ_{AVRG} results in accordingly smaller H_c values. The H_c vs. σ_{AVRG} relation in this range has a linear trend (dashed line, Fig. 3B). This is not surprising since reduced stress levels in the CoFe films result in smaller contribution of the magnetoelastic anisotropy energy to the overall anisotropy energy and thus, the smaller coercivity of CoFe films with lower stress levels is expected. However, the CoFe films with stress level below 130×10^6 Pa show a sudden increase in H_c values. This cannot be attributed to the stress related magnetic anisotropy change. The plausible explanation for this dependence could be found in more detailed consideration of the additive incorporation phenomenon [3]. The magnetic decoupling of the CoFe grains due to additive related inclusion precipitation on the grain boundaries is an antagonistic effect on coercivity of the CoFe films. The two seemingly opposite effects of saccharin on coercivity of CoFe films result in the observed minimum in H_c vs. σ_{AVRG} dependence i.e. an optimum saccharin concentration producing the CoFe films with the lowest coercivity values.

5. Saccharin effect on morphology of CoFe films and nanostructures

The additives are traditionally associated with the highly reflective appearance of the electrodeposit. This effect is described through the reduction of surface roughness and different criteria and characterization methods are employed to quantify it. In Fig. 4A the effect of saccharin on the resulting surface roughness of electrodeposited CoFe films is illustrated. The surface roughness evolution (w) is measured over the increasing length scale for $1.0 \mu\text{m}$ thick CoFe films. They are electrodeposited from solutions containing 0.12 g L^{-1} , 1 g L^{-1} and 2 g L^{-1} of saccharin [39,40]. The observed saturation roughness of CoFe films is decreasing function of saccharin concentration; $w_{\text{sat}} (0.12 \text{ g L}^{-1}) < w_{\text{sat}} (1 \text{ g L}^{-1}) < w_{\text{sat}} (2 \text{ g L}^{-1})$. The additional analysis of this data is presented in inset of Fig. 4A. The saturation roughness is correlated with the sulfur/saccharin incorporation. The correlation between the w_{sat} and R_s shows decreasing logarithmic trend implying that additive incorporation phenomenon has important consequence for the CoFe film surface morphology control. The complete phenomenological description of saccharin effect on surface roughness of CoFe

films is not present at this moment and it certainly represents an open question for future scientific debate.

Knowing the optimum saccharin concentration in the solution is particularly important when electrodeposition of CoFe nanostructures is considered. The role of saccharin to control nanostructure morphology becomes very important at nanoscale electrode geometry [6,43]. For illustration purpose, the surface finish of the two CoFe nanostructures produced from solutions with different saccharin concentrations is shown in the Fig. 4B and C. The small alteration in saccharin concentration yields significantly different outlook of the CoFe nanostructures. This emphasizes the importance of saccharin formulation for overall control of the magnetic nanostructures morphology.

6. Saccharin effect on corrosion potential of CoFe films

Sulfur incorporation in the electrodeposited CoFe films represents a great problem when corrosion properties are evaluated [14,15,19,41,42]. The electrodeposited CoFe films have corrosion potentials several hundred mV more negative than ones produced by physical deposition methods [43]. This indicates significantly higher corrosion susceptibility which could be detrimental obstacle for their application in future magnetic devices [1,3].

The example of saccharin effect on the corrosion properties of CoFe films is shown in Fig. 5. The noblest CoFe surface with the most positive corrosion potential, $E_c \approx -0.17$ V, is the one electrodeposited from saccharin-free solution (0.09 at% S, Fig. 5A). The surface of CoFe films electrodeposited from solution containing 0.12 g L^{-1} of saccharin (0.78 at% S, Fig. 5A) has the most negative corrosion potential, $E_c \approx -0.6$ V. The sample electrodeposited from the solution containing 2 g L^{-1} of saccharin (0.43 at% S, Fig. 5A) has the corrosion potential $E_c \approx -0.35$ V. The incorporation rate of sulfur and corresponding S-content in the CoFe matrix for the 0.12 g L^{-1} sample is ≈ 2 times larger than for the 2 g L^{-1} sample and ≈ 8 times larger than for the 0 g L^{-1} sample. This reflects on the corrosion potential indicating the poorest corrosion resistance of this sample. In Fig. 5A, inset, the CoFe alloy corrosion potential is presented as a function of saccharin/sulfur incorporation rate. The decreasing linear trend is evident.

The electrochemical measurements unambiguously indicate that samples with higher content of sulfur and larger sulfur incorporation rates are also the ones that will corrode faster [15].

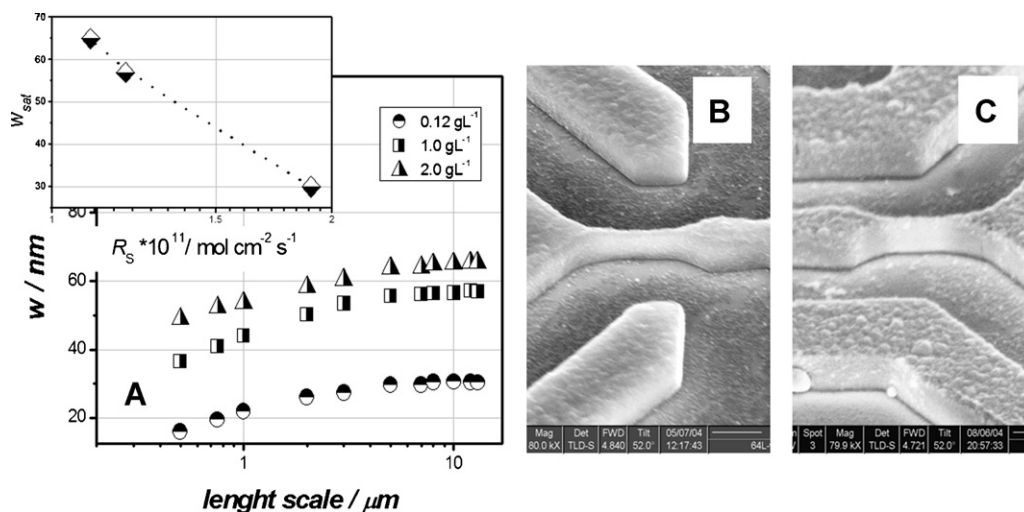


Fig. 4. (A) The CoFe alloy surface roughness as a function of the length scale for different concentration of saccharin. (B) The CoFe nanostructure obtained from solution containing 0.12 g L^{-1} and (C) 2 g L^{-1} of saccharin. Inset in (A) shows the saturation roughness dependence on sulfur/saccharin incorporation rate [43]. The electrodeposition condition and solution are: $0.1 \text{ M FeSO}_4 + 0.05 \text{ M CoSO}_4 + 0.3 \text{ M NH}_4\text{Cl} + 0.4 \text{ M H}_3\text{BO}_3$, $\text{pH} = 2.1$. $\omega = 300 \text{ rpm}$ and $j = 4 \text{ mA cm}^{-2}$. The CoFe films are deposited on polycrystalline Cu disks.

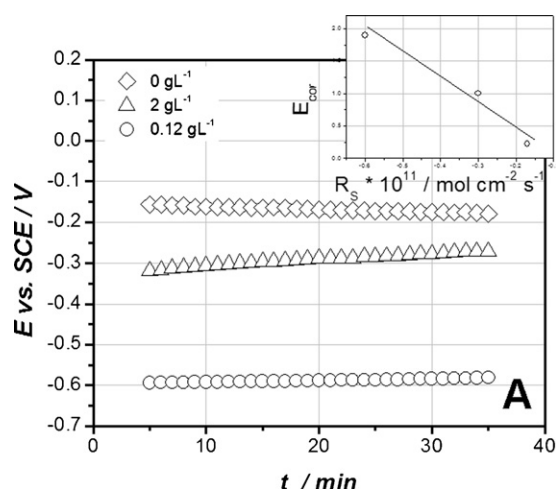


Fig. 5. The corrosion potential transients for CoFe films electrodeposited from solutions having different saccharin concentrations. The inset shows the corrosion potential dependence on sulfur/saccharine incorporation rate. The test solution is 0.05 M NaCl [20]. The details of the deposition process and solution design are: 0.1 M FeSO_4 + 0.05 M CoSO_4 + 0.3 M NH_4Cl + 0.4 M H_3BO_3 , pH = 2.1. ω = 300 rpm and j = 4 mA cm^{-2} . The CoFe films are deposited on polycrystalline Cu disks.

However, the larger incorporation rates of sulfur lead to softer CoFe films with generally lower stress level. The optimum design of the saccharin content has to consider both effects. This could be done with a help of the dimensionless criterion based on the ratio between achieved decrease in coercivity with addition of saccharin in the solution and the corresponding relative increase in corrosion rate [20]:

$$\mathfrak{R} = \frac{H_{c,0}}{H_c(c_{\text{sac}})} \cdot \frac{j_0}{j(c_{\text{sac}})} \quad (5)$$

Here, $H_{c,0}$, and $H_c(c_{\text{sac}})$ are coercivity of the electrodeposited films from solution without and with saccharin. The j_0 and $j(c_{\text{sac}})$ terms represent the corrosion currents (rates) of the films electrodeposited from solutions without and with saccharin.

The $H_{c,0}/H_c(c_{\text{sac}})$ ratio is always >1. The $j_0/j(c_{\text{sac}})$ ratio is calculated using the measured corrosion potentials and taking the oxygen reduction as the representative cathodic reaction during CoFe alloy corrosion [44]. The \mathfrak{R} value is then easily calculated (\mathfrak{R} = 0.14 for 2 g L^{-1} sample and \mathfrak{R} = 0.00075 for 0.12 g L^{-1} sample). The \mathfrak{R} values <1 are always observed for the CoFe films electrodeposited from saccharin containing solutions. This means that the benefit of saccharin in achieving lower coercivity is relatively smaller than the corresponding increase in CoFe alloy corrosion rate. One way to improve this situation is to incorporate a small amount of noble metal (1–2 at%) into the alloy [6,45,46]. This increases the absolute value of the work function of the CoFe alloy and the energy barrier for charge transfer resulting in a lower corrosion rates. The recent reports indicate that the noble metals from the Pt group are the natural choice for alloying with CoFe [6,45].

7. Conclusions

The new challenges in electrodeposition of magnetic films stress the importance of saccharin and other additives for control of the properties and morphology of magnetic films and nanostructures. The conditions at the electrochemical interface for saccharin adsorption, coverage and incorporation become critically important to obtain CoFe films with optimum properties. Understanding and defining the proper phenomenological relation between the

saccharin concentration and resulting properties of CoFe films is pivotal for successful design of electrodeposition process and its integration in manufacturing of the future magnetic devices. Undoubtedly, the design of new and more effective additives for electrodeposition of CoFe films will be the one of the main research directions in the near future.

Acknowledgment

The National Science Foundation, Division of Electrical, Communications and Cyber Systems supported this research, ECCS-0824215.

References

- [1] E.I. Cooper, C. Bonhote, J. Heidmann, Y. Hsu, P. Kern, J.W. Lam, M. Ramasubramanian, N. Robertson, L.T. Romankiw, H. Xu, IBM Journal of Research and Development 49 (103) (2005).
- [2] W. Ehrfeld, *Electrochimica Acta* 48 (2003) 2857.
- [3] S.R. Brankovic, N. Vasiljevic, N. Dimitrov, in: M. Paunovic, M. Schlesinger (Eds.), *Applications to Magnetic Recording and Microelectronic Technologies*, Modern Electroplating, V, John Wiley and Sons Inc., 2010, p. 573 (Chapter 27).
- [4] X.M. Yang, H. Gentile, A. Eckert, S.R. Brankovic, *Journal of Vacuum Science & Technology B* 22 (2004) 3339.
- [5] X.M. Yang, A. Eckert, K. Mountfield, H. Gentile, C. Seiler, S.R. Brankovic, E. Johns, *Journal of Vacuum Science & Technology B* 21 (2003) 3017.
- [6] S.R. Brankovic, X.M. Yang, T.J. Klemmer, M. Seigler, *IEEE Transactions on Magnetics* 42 (132) (2006).
- [7] L.T. Romankiw, D.A. Thompson, US Patent 4,295,173 (1981).
- [8] N. Robertson, H.L. Hu, C. Tsang, *IEEE Transactions on Magnetics* 33 (1997) 2818.
- [9] I. Tabakovic, S. Riemer, V. Inturi, P. Jallen, A. Thayer, *Journal of the Electrochemical Society* 147 (2000) 219.
- [10] T. Osaka, M. Takai, K. Hayashi, K. Ohashi, M. Saito, K. Yamada, *Nature* 392 (1998) 796.
- [11] T. Osaka, T. Yokoshima, D. Shiga, K. Imai, K. Takashima, *Electrochemical and Solid State Letters* 6 (2003) C53.
- [12] T. Osaka, T. Sawaguchi, F. Mizutani, T. Yokoshima, M. Takai, Y. Okinaka, *Journal of the Electrochemical Society* 146 (1999) 3295.
- [13] B.N. Popov, K.-M. Yin, R.E. White, *Journal of the Electrochemical Society* 140 (1993) 1321.
- [14] I. Tabakovic, J. Gong, S. Riemer, V. Venkatasamy, M. Kief, *Electrochimica Acta* 55 (2010) 9035.
- [15] S. Riemer, J. Gong, M. Sun, I. Tabakovic, *Journal of the Electrochemical Society* 159 (2009) D439.
- [16] S.R. Brankovic, N. Vasiljevic, T.J. Klemmer, E.C. Johns, *Journal of the Electrochemical Society* 152 (2005) C196.
- [17] J. Edwards, *Transactions of the Institution of Metal Finishing* 39 (1962) 52.
- [18] S.R. Brankovic, R. Haislmaier, N. Vasiljevic, *Electrochemical and Solid State Letters* 10 (2007) D67.
- [19] T. Osaka, M. Takai, Y. Sogawa, T. Momma, K. Ohashi, M. Saito, K. Yamada, *Journal of the Electrochemical Society* 146 (1999) 2092.
- [20] J. George, S.-E. Bae, D. Litvinov, J. Rancher, S.R. Brankovic, *Journal of the Electrochemical Society* 155 (2008) D589.
- [21] G.S. Frankel, V. Brusic, R.G. Schad, J.W. Chang, *Corrosion Science* 35 (1993) 63.
- [22] H. Kwon, A.A. Gewirth, *Journal of the Electrochemical Society* 154 (2007) D577.
- [23] C. Buessherman, *Progress in Surface Science* 46 (1994) 335.
- [24] B.B. Damaskin, O.A. Petri, V.V. Batrakov, *Adsorption of Organic Compounds on Electrodes*, Plenum Press, New York, 1971, p. 259.
- [25] J.O'M. Bockris, A.K.N. Reddy, *Modern Electrochemistry II*, Plenum Press, New York, 1970, p. 791.
- [26] C.H. Hamann, A. Hamnett, W. Vielstich, *Electrochemistry*, Wiley-VCH, New York, 1998, p. 187.
- [27] W. Bang, K. Hong, *Electrochemical and Solid State Letters* 10 (2007) J86.
- [28] I. Tabakovic, V. Inturi, S. Riemer, *Journal of the Electrochemical Society* 149 (2002) C18.
- [29] H.V. Venkatasetty, *Journal of the Electrochemical Society* 117 (1970) 403.
- [30] J. George, *Electrochemical synthesis of magnetic materials for magnetic recording and MEMS application*, Ph.D. Thesis, University of Houston, December 2012, p. 150.
- [31] S.R. Brankovic, B. Kagajwala, J. George, G. Majkic, G. Stafford, *Electrochimica Acta* (2012), accepted.
- [32] O.E. Kongstein, U. Bertocci, G.R. Stafford, *Journal of the Electrochemical Society* 152 (2005) C116.
- [33] G.G. Stoney, *Proceedings of the Royal Society of London* 82 (1909) 172.
- [34] S.C. Seel, C.V. Thompson, S.J. Hearne, *Journal of Applied Physics* 88 (2000) 7019.
- [35] R.W. Hoffman, *Thin Solid Films* 34 (1976) 185.
- [36] W.D. Nix, B.M. Clemens, *Journal of Materials Research* 14 (1999) 3467.

- [37] C.V. Thompson, *Journal of Materials Research* 14 (1999) 3164.
- [38] L.B. Freund, E. Chason, *Journal of Applied Physics* 89 (2001) 4866.
- [39] S.R. Brankovic, J. George, S.-E. Bae, D. Litvinov, *Electrochemical Society Transactions* 16 (2009) 75.
- [40] S.R. Brankovic, N. Vasiljevic, in: S. Krongelb, C. Bonhote, S.R. Brankovic, Y. Kitamoto, T. Osaka, W. Schwarzhacher, G. Zangari (Eds.), *Magnetic Materials Processes and Devices VIII*, 2006, p. 397, PV 2004-23.
- [41] L. Ricq, F. Lallemand, M.P. Gigandet, J. Pagetti, *Surface and Coatings Technology* 138 (2001) 278.
- [42] F. Lallemand, L. Ricq, P. Bercot, J. Pagetti, *Electrochimica Acta* 47 (2002) 4149.
- [43] S.R. Brankovic, R. Haislmaier, N. Vasiljevic, *Electrochemical Society Transactions* 3 (2007) 71.
- [44] V. Jovancevic, J.O.M. Bockris, *Journal of the Electrochemical Society* 133 (1986) 1797.
- [45] I. Tabakovic, S. Riemer, M. Sun, V. Vas'ko, J. Qui, M. Kief, *Electrochemical Society Transactions* 3 (2007) 47.
- [46] Q. Huang, C. Bonhote, J. Lam, L.T. Romankiw, *Electrochemical Society Transactions* 3 (2007) 61.